Mechanistic details of the formation and growth of nanoscale voids in Ge under extreme conditions within an ion track

Hooda, Sonu

2017-06-07

Hooda , S , Avchachov , K , Khan , S A , Djurabekova , F , Satpati , B , Nordlund , K , Bernstorff , S , Ahlawat , S , Kanjilal , D & Kabiraj , D 2017 , ' Mechanistic details of the formation and growth of nanoscale voids in Ge under extreme conditions within an ion track ' , Journal of Physics. D, Applied Physics , vol. 50 , no. 22 , 225302 . https://doi.org/10.1088/1361-6463/aa6e25

http://hdl.handle.net/10138/308772
https://doi.org/10.1088/1361-6463/aa6e25

Preprint of paper published as Journal of Physics. D, Applied Physics. 50, 22 (2017) 225302.

Mechanistic details of the formation and growth of nanoscale voids in Ge under extreme conditions within an ion track

Sonu Hooda[1], Konstantin Avchachov[2], S. A. Khan[1], Flyura Djurabekova[2], Kai Nordlund[2], B. Satpati[3], Sigrid Bernstorff[4], Sarita[5], D. Kanjilal[1], D. Kabiraj[1]

[1]*Inter-University Accelerator Centre, Aruna Asaf Ali Marg, New Delhi-110067, India*

[2] *Saha Institute of Nuclear Physics, 1/AF, Bidhannagar, Kolkata-700064, India*

[3]*Department of Physics and Helsinki Institute of Physics, University of Helsinki, 00014 Helsinki, Finland*

[4]*Sincrotrone Trieste, SS 14 km163,5, 34012 Basovizza, Italy*

[5]*Bhabha Atomic Research Centre, Mumbai 400 085, India*

Abstract

The initial steps of Ge nanovoids formation have been studied. Two step energetic ion irradiation processes was used to fabricate novel and distinct embedded nanovoids within bulk Ge. The formation of voids in amorphous-Ge (a-Ge) and their size, and shape evolution under ultra-fast thermal spike within ion track of swift heavy ion, is meticulously expatiated using experimental and theoretical approaches. The 'bow-tie' shape of void formed in single ion track tends to attain spherical shape as the ion tracks overlap at about 1×10^{12} ions cm^{-2} and the void assumes prolate spheroid shape with major axis along the ion trajectory at sufficiently high ion fluences. Small angle X-ray scattering can provide information about primary stage of void formation hence this technique is applied for monitoring simultaneously their formation and growth dynamics. The results are supported by transmission (XTEM) and scanning (XSEM) electron micrographs. The multi-time-scale theoretical approach corroborate the experimental findings and relate the bow-tie shape void formation to density variation as a result of melting and resolidification of Ge within thermal spike generated along ion track plus non-isotropic stresses generated towards the end of the thermal spike.

Introduction

different particles scatter X-rays independently and their sum gives the total scattering intensity. Since the voids are randomly distributed and there may be a size distribution as well, we use assumption of poly-dispersed particles. The GISAXS data were analysed using the software SASFIT [34]. To analyse the contribution from open volume with different shapes in the resultant scattered intensity, the form factor *F (q)* for different shapes like plate, cylinder and sphere were used for best fit of the data. The solid lines are fits to the spectra using the software as described above. Since the scattering measurements are performed in reciprocal space, the larger size inhomogeneities are contributing to scattered intensity at lower q region and vice versa. The described method revealed the average shape and size of voids as given in the table below.

Figure 3. Fitted line profile from the GISAXS data along (a) q_y for same q_z width and; (b) q_z for same q_y

Table. Size and shape of voids extracted from GISAXS data after fitting

Ion fluence (ions cm^{-2})	**Dimension of the voids (nm)**		**Shape of voids**
	Out-of-plane	**In-plane**	
1×10^{11}	10.2	4.2	Plate
5×10^{11}	11	4.5	Plate
1×10^{12}	16.8	16.8	Sphere
5×10^{12}	22	22	Sphere
1×10^{13}	26	26	Sphere

As can be seen from Table 1, the ion irradiation creates plates like voids which are actually bow-tie shaped as described in the next section. The ion passing nearby these voids, as the fluence increases, increased their volume and change the shape. At about 1×10^{12} ions/cm^2, the voids assume spherical shape as the ion tracks are expected to overlap. With further increase in fluence, their diameter is found to increase from this analysis.

2.

Discussion

The c-Ge was observed to be insensitive to ionizing part of deposited energy from 100 MeV Ag ions. However, the irradiation of a-Ge with same ion leads to remarkable structural modifications. The void formation in a-Ge, after Ag ions irradiation can be understood on the basis of inelastic thermal spike model (I-TS) which describes SHI interactions with matter [35]. The target can be divided in two subsystems (i) the electronic and (ii) the lattice subsystem. The energy of incident Ag ion is shared between the target electrons. This energy stored in the electronic system is transferred to the atomic system via electron–phonon (e-p) coupling which finally leads to a transient rise in temperature locally. The electrons are confined within a cylindrical track along ion path and their confinement has strong influence on e-p coupling strength (g). Here, I-TS is used to describe the rise in temperature of lattice. The detailed description of two temperature model is given in our previous reports[20-22], where the temperature rise, formation of track and diameter of track were calculated in c-Ge and a-Ge. In case of c-Ge, the value of '*g*' is low enough such that 100 MeV Ag produce no lattice defects that corroborate the results showing insensitivity of c-Ge towards S_e. Whereas in a-Ge, it leads to molten track formation with diameter~10 nm. Consequently, melting and re-solidification with efficient e-p coupling results in void formation due to higher density of Ge in liquid phase as compared to solid phase [13] which is inferred from the molecular dynamics simulation discussed in following sub-section.

Molecular Dynamics Simulations

Molecular dynamics (MD) simulations, using PARCAS code[36], were performed to get insight of void formation within ion track and modification of existing voids by multiple overlap of these tracks. The results from simulations demonstrating formation of bow-tie shaped voids in a-Ge due to single ion impact have been reported earlier[13]. The simulations have been extended here to study the effect of subsequent ion track on the shape and size of these bow-tie shaped voids. The volume of the simulation cell was 61×41×41 nm^3 having about 4.5 million germanium atoms which were initially arranged on c-Ge lattice. This c-Ge simulation cell was transformed into a-Ge by the approach introduced by Wooten et al.[37].

As discussed earlier, the impact of SHI can locally and transiently melt the a-Ge around its trajectory. Since Ge has higher density in liquid state as compared to solid state, this means that SHI can produce transient density changes from low to high during melting and vice versa on re-solidification. Therefore, the MD simulations should ideally use potentials which can accurately describe the solid to liquid and liquid to solid phase transformations in Ge. Since no

single potential served the purpose as described in Supplemental Material of reference [13], Posselt Stillinger-Weber potential [38] was used for simulations during the first 100 ps after the ion passage and Tersoff potential [39] for later time. The simulation cell had 0.6 nm wide border region in x and y directions, temperature controlled at 300 K by Berendsen thermostat[40], to cool down the heat spike generated sound/heat wave at the boundaries and thereby suppressing their reflection back to the centre of the cell.

The simulation of effect of SHI interaction with matter has to take care of several different processes like excitation of electrons accounting for the electronic stopping power and atomic displacements due to nuclear stopping power. Since nuclear stopping power is several orders smaller in comparison of electronic stopping power of 100 MeV Ag ions in Ge, the simulations account for excitation of electrons. The columbic interaction between nuclear charge of projectile with bound and free electrons in medium produce energetic electrons named as δ-electrons. These electrons have energies up to tens of eV and they scatter with lattice atoms as they travel in the material, thereby exciting additional electrons into the conduction band (impact ionization). Consequently, these energetic electrons thermalize by multiple scattering to reduce their energy to ~ 5 eV and emit phonons by electron-phonon coupling. In this work, the dynamics of excited electrons was handled using a combination of asymptotical trajectory Monte Carlo (MC) approach and two-temperature model (TTM). The MC method was used to model the dynamics of the excited electrons, having kinetic energy ≥ 5eV, which travel through the a-Ge and take part in impact ionization and electron-hole pair recombination through Auger processes. TTM, on the other hand, was used to treat the electrons, with kinetic energy 5 eV, which take part in electron-phonon coupling process. The details of TTM and the values of the related parameters can be found in the Supplement Material of reference [13]. It may be noted here that the high energy electrons treated by MC method lose their energy and start participating in electron-phonon coupling process. Therefore, the two processes MC and TTM methods cannot be performed sequentially but rather a synchronized MC-TTM approach is applied. The MC-TTM approach was applied up to 30 ps after the ion passage to extract the electron-phonon energy exchange rates which were then used as inputs to the MD simulations. The MD simulations are performed till 300 ps after an ion impact. The snapshot from the simulations is shown in Figure 5. The red broken curve shows the cross-sectional view of the void created by the first impacting ion which resembles a bow-tie in agreement with the experimentally observed shape of a void shown in Figure 4(a). In the same volume, the effect of second ion was simulated and followed for 300 ps again. The black broken curve outlines the resulting shape of the void due to the second impact. As can

be seen from Figure 5, the second impact increased the size of the existing void more prominently in the axial direction.

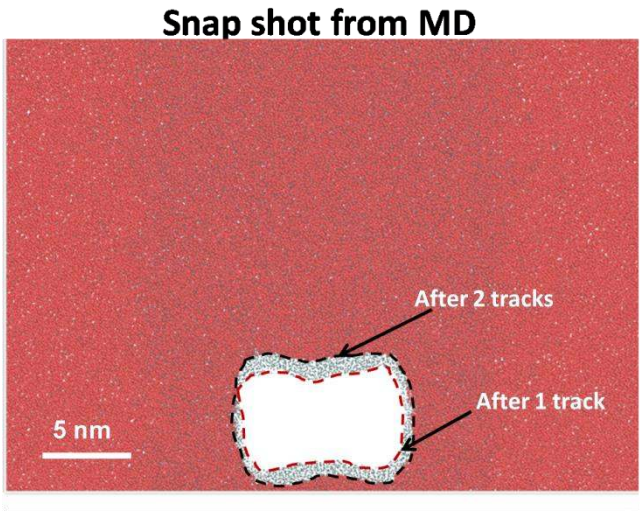

Figure 5. Superimposed snapshots from MD simulations of two consecutive 100 MeV Ag ion impacts in the centre of the simulation cell. The projection of ion trajectory is along top to bottom of the image. The volume in white is created by the first incident ion. The atoms depicted by grey circles were displaced during the heat spike generated by the second incident ion.

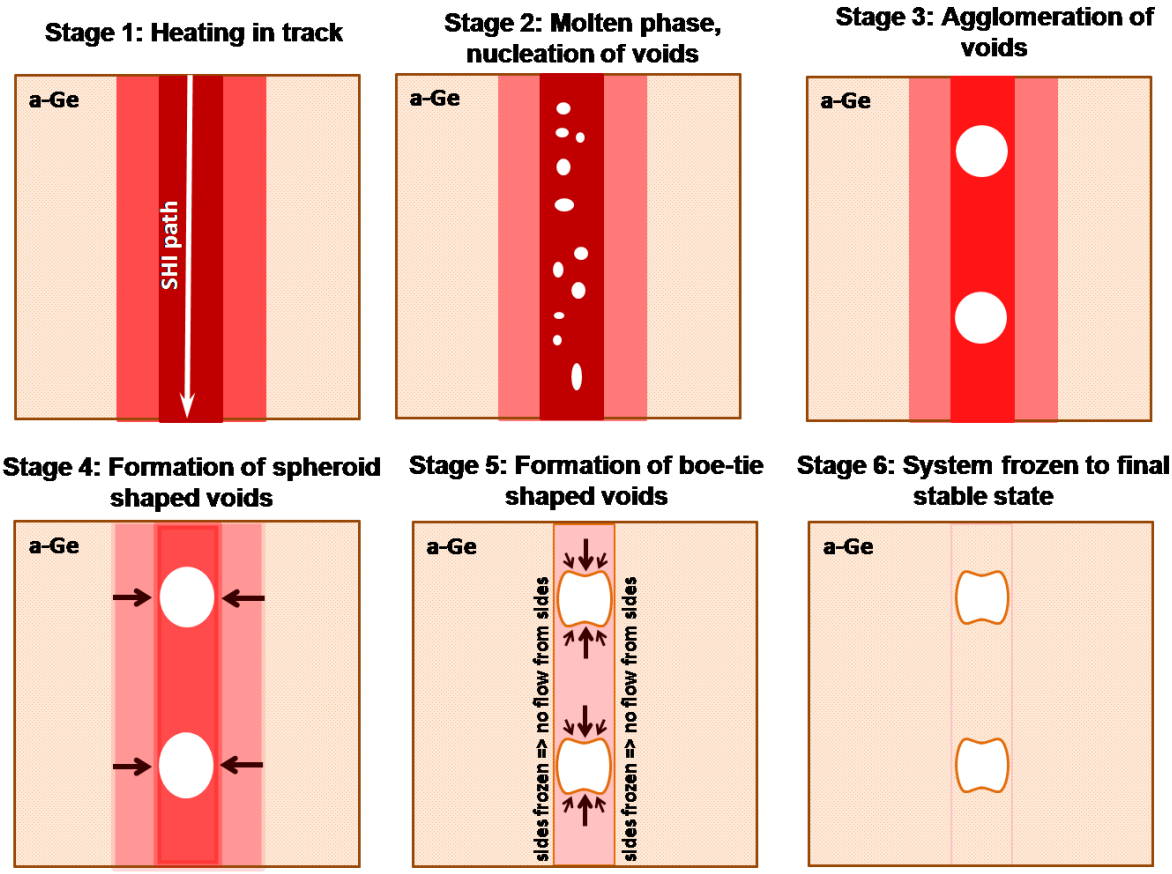

Figure 6. The schematic of various stages included in formation of void in the ion track

With the help of schematic diagram as shown in figure 6, we tried to explain bow-tie shaped void formation as proposed by Ridgway *et al.* [13]. In stage 1, as the ion passes through the material and a high temperature zone is created with Gaussian temperature distribution radially around the ion path. The thermal spike produces a radially outward material flow from the ion-track core and a phase transformation from low density solid to high density liquid in the core. In stage 2, a cylindrical molten zone is formed where voids nucleate due to higher density of Ge in liquid phase (l-Ge) as compared to Ge in solid phase. In stage 3, the small voids agglomerate to form bigger voids. When the track starts to cool, the cooling occurs from outside to inside radially in the track. In stage 4, the resolidified Ge with higher volume exerts radially inwards force which changes the shape of the voids to prolate spheroids. Arrows in the schematic indicates the direction of force. In stage 5, the expansion surrounding the still molten central volume pushes the molten material in the axial direction of the void which changes its shape to bow-tie. Finally the system freezes in this state and we observe the bow-tie shaped voids due to single ion impact, as shown in figures 5 and 4(a), with the help of MD and TEM image.

Due to multiple ion impact or overlapping of ion tracks the size of bow-tie shaped void increases as shown with the help of MD results in figure 5(a). However, the increase in size is prominent along the axial direction of ion path as compared to the radial direction. This is clear from the snapshot of MD after overlapping ion track. This axial increase in void size continues with subsequent ion track overlaps as the fluence is increased which results in a transition from bow tie- to sphere as a function of ion fluence. Moreover, it results in formation of bigger voids assuming shape of prolate spheroid on further increasing the ion fluences as discussed in our previous reports [3,14]. The shape and size evolution is estimated with the help of GISAXS results and further corroborated with the help of microscopy (XTEM and XSEM) results at higher ion fluences.

Conclusion

Swift heavy ions can induce porosity in damaged Ge as a result of void formation. The shape of the voids changes and their volume increases as the ion fluence is increased. The generation of voids in damaged Ge and their structural transformation is studied here using experimental and theoretical approaches. Experimental results, derived from XTEM, XSEM and GISAXS

investigations, showed that the shape of voids is bow-tie like at initial fluences which tends towards spherical shape as the ion tracks overlap at about 1×10^{12} ions cm^{-2}. With further increase in fluence, the voids take prolate spheroid shape with major axis along the ion trajectory. The multi-time-scale theoretical approach comprising of an asymptotical trajectory MC calculation of the electron dynamics, a TTM description of the heat dissipation and a MD simulation shed insight into the process of void formation and subsequent shape transformation. The theoretical results corroborate the experimental findings and relate the bow-tie shape to density fluctuation around ion trajectory as a result of thermal spike created in the material and non-isotropic stresses generated towards the end of the thermal spike.

Acknowledgements

[1] D. Sun, A. E. Riley, A. J. Cadby, E. K. Richman, S. D. Korlann, and S. H. Tolbert, Nature **441**, 1126 (2006).
[2] J. Shieh, H. L. Chen, T. S. Ko, H. C. Cheng, and T. C. Chu, Advanced Materials **16**, 1121 (2004).
[3] S. Hooda, S. A. Khan, B. Satpati, A. Uedono, S. Sellaiyan, K. Asokan, D. Kanjilal, and D. Kabiraj, Microporous and Mesoporous Materials **225**, 323 (2016).
[4] H. Föll, J. Carstensen, and S. Frey, J Nanomater **2006**, 10, 91635 (2006).
[5] G. Kaltsas and A. G. Nassiopoulou, Sensors and Actuators A: Physical **76**, 133 (1999).
[6] H. Goldsmid, Materials **2**, 903 (2009).
[7] N. G. Rudawski, B. L. Darby, B. R. Yates, K. S. Jones, R. G. Elliman, and A. A. Volinsky, Appl. Phys. Lett. **100** (2012).
[8] E. G. Rojas, H. Plagwitz, B. Terheiden, J. Hensen, C. Baur, G. La Roche, G. Strobl, and R. Brendel, Journal of the Electrochemical Society **156**, D310 (2009).
[9] T. S. Ko, J. Shieh, M. C. Yang, T. C. Lu, H. C. Kuo, and S. C. Wang, Thin Solid Films **516**, 2934 (2008).
[10] M. Christophersen, S. Langa, J. Carstensen, I. Tiginyanu, and H. Föll, physica status solidi (a) **197**, 197 (2003).
[11] H. Föll, M. Leisner, A. Cojocaru, and J. Carstensen, Materials **3**, 3006 (2010).
[12] T. Steinbach, J. Wernecke, P. Kluth, M. C. Ridgway, and W. Wesch, Phys. Rev. B **84**, 104108 (2011).
[13] M. C. Ridgway *et al.*, Physical Review Letters **110**, 245502 (2013).
[14] S. Hooda, S. A. Khan, B. Satpati, D. Stange, D. Buca, M. Bala, C. Pannu, D. Kanjilal, and D. Kabiraj, Appl. Phys. A **122**, 1 (2016).
[15] R. Böttger, K.-H. Heinig, L. Bischoff, B. Liedke, and S. Facsko, Appl. Phys. A **113**, 53 (2013).
[16] T. Steinbach, C. S. Schnohr, P. Kluth, R. Giulian, L. L. Araujo, D. J. Sprouster, M. C. Ridgway, and W. Wesch, Phys. Rev. B **83**, 054113 (2011).
[17] B. Roman, K. Adrian, B. Lothar, and F. Stefan, Nanotechnology **24**, 115702 (2013).
[18] S. A. Mollick, D. Ghose, and B. Satpati, Vacuum **99**, 289 (2014).
[19] K. Gärtner, J. Jöhrens, T. Steinbach, C. S. Schnohr, M. C. Ridgway, and W. Wesch, Phys. Rev. B **83**, 224106 (2011).
[20] S. Hooda, B. Satpati, T. Kumar, S. Ojha, D. Kanjilal, and D. Kabiraj, RSC Advances (2015).
[21] S. Hooda, B. Satpati, S. Ojha, T. Kumar, D. Kanjilal, and D. Kabiraj, Materials Research Express **2**, 045903 (2015).
[22] S. Hooda, S. A. Khan, B. Satpati, D. Kanjilal, and D. Kabiraj, Appl. Phys. Lett. **108**, 201603 (2016).
[23] D. Sarker, H. Kumar, R. Patra, D. Kabiraj, D. K. Avasthi, S. K. Vayalil, S. V. Roth, P. Srivastava, and S. Ghosh, J Appl Phys **115**, 174304 (2014).
[24] S. Yu *et al.*, The Journal of Physical Chemistry C **119**, 4406 (2015).
[25] S. Koyiloth Vayalil, A. Gupta, S. V. Roth, and V. Ganesan, J Appl Phys **117**, 024309 (2015).
[26] I. D. Desnica-Franković, P. Dubcek, U. V. Desnica, S. Bernstorff, M. C. Ridgway, and C. J. Glover, Nucl. Instr. Meth. Phys. Res. B **249**, 114 (2006).
[27] J. F. Ziegler, M. D. Ziegler, and J. P. Biersack, Nucl. Instr. Meth. Phys. Res. B **268**, 1818 (2010).
[28] H. Amenitsch, M. Rappolt, M. Kriechbaum, H. Mio, P. Laggner, and S. Bernstorff, Journal of synchrotron radiation **5**, 506 (1998).
[29] G. Benecke *et al.*, Journal of Applied Crystallography **47**, 1797 (2014).
[30] Y. Yoneda, Physical Review **131**, 2010 (1963).
[31] K. Devloo-Casier, K. F. Ludwig, C. Detavernier, and J. Dendooven, Journal of Vacuum Science & Technology A **32**, 010801 (2014).
[32] M. Schwartzkopf *et al.*, Nanoscale **5**, 5053 (2013).
[33] V. A. Raghunathan, Resonance **10**, 24 (2005).
[34] I. Bressler, J. Kohlbrecher, and A. F. Thunemann, J. Appl. Crystallogr. **48**, 1587 (2015).
[35] M. Toulemonde, C. Dufour, and E. Paumier, Phys. Rev. B **46**, 14362 (1992).

[36] K. Nordlund, M. Ghaly, R. S. Averback, M. Caturla, T. Diaz de la Rubia, and J. Tarus, Phys. Rev. B **57**, 7556 (1998).
[37] F. Wooten, K. Winer, and D. Weaire, Phys. Rev. Lett. **54**, 1392 (1985).
[38] M. Posselt and A. Gabriel, Physical Review B **80**, 045202 (2009).
[39] J. Tersoff, Physical Review B **39**, 5566 (1989).
[40] W. C. D. Cheong and L. C. Zhang, Nanotechnology **11**, 173 (2000).